International Journal of Concrete Structures and Materials

RESEARCH Open Access

Experimental Evaluation on Blast Resistance of Reinforced Concrete Structures under Partially Confined Explosion

Youngjun Park[1], Kukjoo Kim[2], Sang-woo Park[3], Sang-Guk Yum[4] and Jang-Woon Baek[5*]

Abstract

As the risk of accidental explosions at ammunition storage or hydrogen charging station increases in populated area, it is needed to design the facilities against blast loading, particularly subjected to partially confined explosion. However, the partially confined explosion lacks experimental test data to efficiently design the facilities subjected to the potential threat, when compared to unconfined or confined explosion cases. As a fundamental study on partially confined explosion, two partially buried tunnel-type structures with normal- and high-strength concretes were tested under a weight charge of 5.9 kg TNT explosion. The major parameters were concrete compressive strength and reinforcement ratio. The test result showed that the damage of the concrete structure with normal-strength concrete was extremely severe, whereas that of the specimen with high-strength was relatively mild. Further, finite element (FE) analyses were performed to investigate the confinement effect of blast load. The FE analysis result showed that under partially confined explosion, the reduction of the maximum displacement by using higher concrete strength was significant, while preventing the failure of the structure. This study provides fundamental data for designing the facilities with explosives subjected to the partially confined explosion.

Keywords Ammunition storage, Hydrogen charging station, Partially confined explosion, Blast design, TNT explosion test, Finite element analysis, AUTODYN software

1 Introduction

Since explosives have been handled by special industries such as military, gas, and firefighting, there has been little concern about explosion threat or protective structures in the private sector. Military facilities with potential risks of accidental explosion such as ammunition storage were originally built outside the city separated from densely populated area. However, as the city has gradually grown with accelerating urbanization, military facilities are predominantly located in urban areas particularly in dense residential area (Choi, 2009). Consequently, the escalating risk of incidental explosions within military facilities and poses an augmented threat to the civilian sector (Buhin, 2016). The substantial damages incurred by the recent explosions of munitions in Kazakhstan and Russia exemplify the outcomes of this heightened risk.

In addition to military facilities, as the technology using hydrogen energy develops in recent years, facilities with potential explosion risks such as hydrogen charging platforms are being located in urban areas (Lin et al., 2020). Recently, an explosion accident

ISSN 1976-0485 / eISSN 2234-1315

*Correspondence:
Jang-Woon Baek
baekjw@khu.ac.kr
[1] Smart Construction Research Group, Hyundai Engineering and Construction, Seoul 03508, South Korea
[2] Protective Structure Analysis Engineer, Defense Installations Agency, Seoul 04353, South Korea
[3] Department of Civil Engineering and Environmental Sciences, Korea Military Academy, Seoul 01805, South Korea
[4] Department of Civil Engineering, Gangneung-Wonju National University, Gangneung 25457, South Korea
[5] Department of Architectural Engineering, Kyung Hee University, Yongin 17104, South Korea

occurred due to oxygen inflow and static electricity in South Korea in 2019, resulting in 8 casualties. Since hydrogen has the characteristics of flammability, low ignition energy, easy leakage and diffusion, and fast flame propagation, the safety has been a major concern in hydrogen applications (Liang et al., 2019). Once hydrogen leaks, either a jet flame or a flammable gas cloud can be formed. With ignition source, explosion can occur in certain cases, and overpressure can damage people and equipment in the hydrogen charging station (Liang et al., 2019).

A number of numerical analyses were performed to simulate the characteristics and risks of hydrogen and gas explosions (Moradi and Groth, 2019). The computational fluid dynamics (CFD) simulations of hydrogen leakage were performed for safety diagnosis of the mobile hydrogen station (Han et al., 2018). The causes of accident related to the hydrogen leakage were analyzed and the simulations were largely divided into external and internal leakage cases. According to the study, the external leakage simulation was relatively safe when compared to internal leakage. Although the process of the hydrogen explosion is different from the conventional explosives, the consequences from the accidental explosives of hydrogens are catastrophic to civilians.

As the potential risk such as the accidental explosion of ammunition storage or hydrogen charging station approaches in dense residential area, it becomes more and more necessary to design those facilities against blast loading, which can severely threaten civilian lives. Such case of accidental explosion of hydrogen charging station can be categorized as partially confined explosion, since the hydrogen tanks are contained in a structure, but the container should have ventilation measures to diminish the significant damages from fully confined explosion.

The magnitude of the explosive loading acting on structures varies according to the confinement of explosive charge. The phenomenon of explosion can be divided into the unconfined explosion and confined explosion, where the confined explosion is further subdivided into fully vented explosion, partially confined explosion, and fully confined explosion (UFC, 2008). When explosion occurs inside a structure, the blast pressure consists of 1) the initial stage where high reflected pressure occurs due to reflected wave within very short duration and 2) the post-peak stage where the high pressure is gradually diminished to the atmospheric pressure due to the interaction between the wave reflected from walls of the structure over various times. As such, for confined explosion, extremely complicated waveforms are generated owing to the combination of the incident wave and the reflected wave rebounded from the structure. The waveforms of the confined explosion last relatively longer when compared to those of unconfined explosion, resulting in more significant damages to the structures (Hung et al., 2020).

For unconfined explosions, several studies have been conducted including several experimental and analytical studies. Hung et al. (2020) carried out C4 explosive tests to evaluate the overpressure response in steel tunnels subjected to external explosions. Through experiments using C4 charge of 2.15 to 3.26 m/kg$^{1/3}$ and hydrodynamic finite element analysis of LS-DYNA, equations for in-tunnel pressure were proposed.

Wang et al., (2012, 2013) performed explosive tests for reinforced concrete one-way slabs subjected to various charge weights of TNT (1, 2, and 3 kg TNT equivalent explosive) close-in explosions to investigate the effects of scale-down factors. The slab dimensions were from 0.75 m×0.75 m×0.03 m to 1.25 m×1.25 m×0.05 m with scaled distance of 0.518 to 0.591 m/kg$^{1/3}$. The major failure modes were spallation damage from a few cracks and moderate spallation damage. As the charge weight of the large-scale slab is increased, the failure mode changed from flexural failure with spall damage on the back surface to perforation failure. The test results were compared with FE analyses performed using LS-DYNA explicit solver. The damage patterns of the test results agreed with those of FE results, indicating that the concrete model of concrete slab under close-in explosion can be predicted by the calibrated FE model using small-scaled test results.

Mendonça et al., (2017, 2018a, 2018b, and 2021) performed extensive unconfined blast test on RC two-way slabs with dimensions of 1.0 m×1.0 m×0.08 m. The reinforcement ratio, concrete strength, and scaled distance were used as major design parameters in the tests. Using the non-confined plastic bonded explosive, the equivalent TNT scaled distance was 1.43 to 1.45 m/kg$^{1/3}$. According to one of the test results (Mendonça et al., 2017), the reinforcement of 0.25% was sufficient to carry the blast load generated at the scaled distance (1.43 to 1.45 m/kg$^{1/3}$). On the other hand, Mendonça et al. (2018b) performed blast tests on 50 MPa concrete slabs with reinforcement ratio of 0.175% in one direction and 0.370% in the perpendicular direction. As the slabs had different reinforcement in mutually perpendicular direction, failure occurred in the direction with lower reinforcing steel with 0.175%.

For fully confined explosions, studies were mainly conducted in the fields of nuclear power plant containment subjected to accidental nuclear explosion (Chen et al., 2010; Dong et al., 2010; Hu & Lin, 2006; Lin et al., 2010; Pandey et al., 2006; Zhao et al., 2012), most of

which focused on the non-linear dynamic finite element analysis.

On the other hand, studies on partially confined explosions are rare, despite the frequent cases of the explosion in urban area (e.g., at a cross roads in proximity to tall building) (Remennikov & Rose, 2005; Smith & Rose, 2006) or the cases of an explosion occurs inside ammunition storage or hydrogen charging station (Liao et al., 2019; Zhi et al., 2019). Edri et al., (2011, 2012) and Feldgun et al. (2012) studied blast pressure analyses due to a partially confined explosion. Different weights of TNT charges (charge weight $W=0.5$, 1.0, 1.5, 2.0, and 4.0 kg with the scaled distance Z of 1.76, 1.40, 1.22, 1.11, and 0.88 m/kg$^{1/3}$, where the standoff distance of $R \approx 1.4$ m toward a wall in the structure was assumed) were detonated in a specially designed composite structure (concrete cast in-between two steel plates). They found out that the gas pressures measured in the test were 27% smaller than the gas pressure predicted by the UFC 3–340-02 model (UFC, 2008). However, since they focused on the blast pressure analysis using the rigid structure that was sufficiently strong to withstand the inner explosion, the damages of the structure were not reported due to the partially confined explosion.

Feldgun et al. (2011) and Feldgun et al. (2016) performed numerical analyses for structures subjected to fully confined or partially confined explosion. Feldgun et al. (2016) showed that a thermodynamic numerical model accounting the afterburning energy and release of explosives within a confined or partially confined air volume predicted well with the test result of the gas pressure. Although the blast pressures under the partially confined explosion were experimentally and analytically investigated, actual experimental responses of a structure under the partially confined explosion were not investigated.

The magnitude of the partially confined explosion can be expected to be greater than that of the unconfined explosion but to be smaller than that of the fully confined explosion. To identify the magnitude of the partially confined explosion, it is needed to carry out experimental tests and to investigate the damage of concrete structures subjected to such explosion. However, actual explosion experiment to reliably simulate effects of explosions is very limited due to security issues on test explosives and test site. Further, the test data for the partially confined explosion are scare due to technical difficulty in simulating testing setup.

As fundamental research on partially confined explosion, small-scaled concrete structures were tested subjected to TNT detonation. To simulate the partially confined explosion, tunnel-type concrete structures were fabricated, and the openings of the structure were closed using steel plates covered by backfilling soil. Further, the FE analysis was performed for different confinement explosion conditions to investigate the effects of partially confined explosion on the damage of the concrete structures.

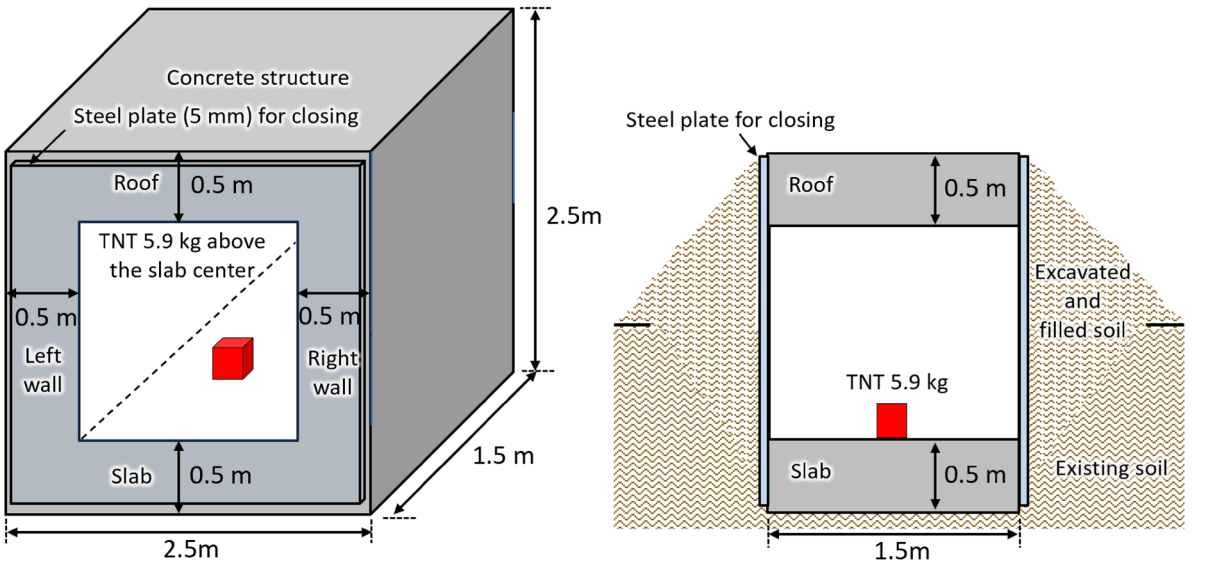

(a) Specimen dimension and instrumentation (b) Explosive loading and boundary conditions of specimen

Fig. 1 Overview of experimental program

2 Test Program

2.1 Design and Fabrication of Specimens

Fig. 1a shows the dimension of tunnel-type specimen. The size of the specimens in length × height × width was 2.5 m × 2.5 m × 1.5 m with the hollow space of 1.5 m × 1.5 m × 1.5 m, simulating a part of concrete structure with the thickness of 0.5 m that may contain ammunition for a magazine or hydrogen tanks for hydrogen charging station. The net explosive charge was determined as 5.9 kg, which is equivalent to the blast load of 152 mm artillery. The scaled distance was 0.415 m/kg$^{1/3}$ toward the left or right wall (i.e., the distance of 0.75 m). According to the design of Technical Manual 5–855 (Army, 1986), qualitative concrete damage can be expected by a given scaled distance and thickness of concrete walls based on empirical test data. The specimen with 0.5-m-thick wall is expected to suffer only a minor crack.

To simulate a partially confined explosion, the openings of the tunnel-type concrete structure were covered by 5-mm-thick steel plates for closing (Fig. 1a), and the structure was buried by backfilling soil to provide supporting pressure to the steel plates (Fig. 1b). To equalize the explosive pressures toward both the openings, the number of soil compaction was carefully controlled so that the soil had 95% the maximum dry density.

Table 1 Test parameters of specimens

Specimen	Design compressive strength of concrete (MPa)	Age of concrete at the day of test (days)		Reinforcement ratio (%)
		Slab	Walls and roof	
NSC	24	27	24	0.306 (D16@175 mm)
HSC	80	27	17	0.559 (D22@175 mm)

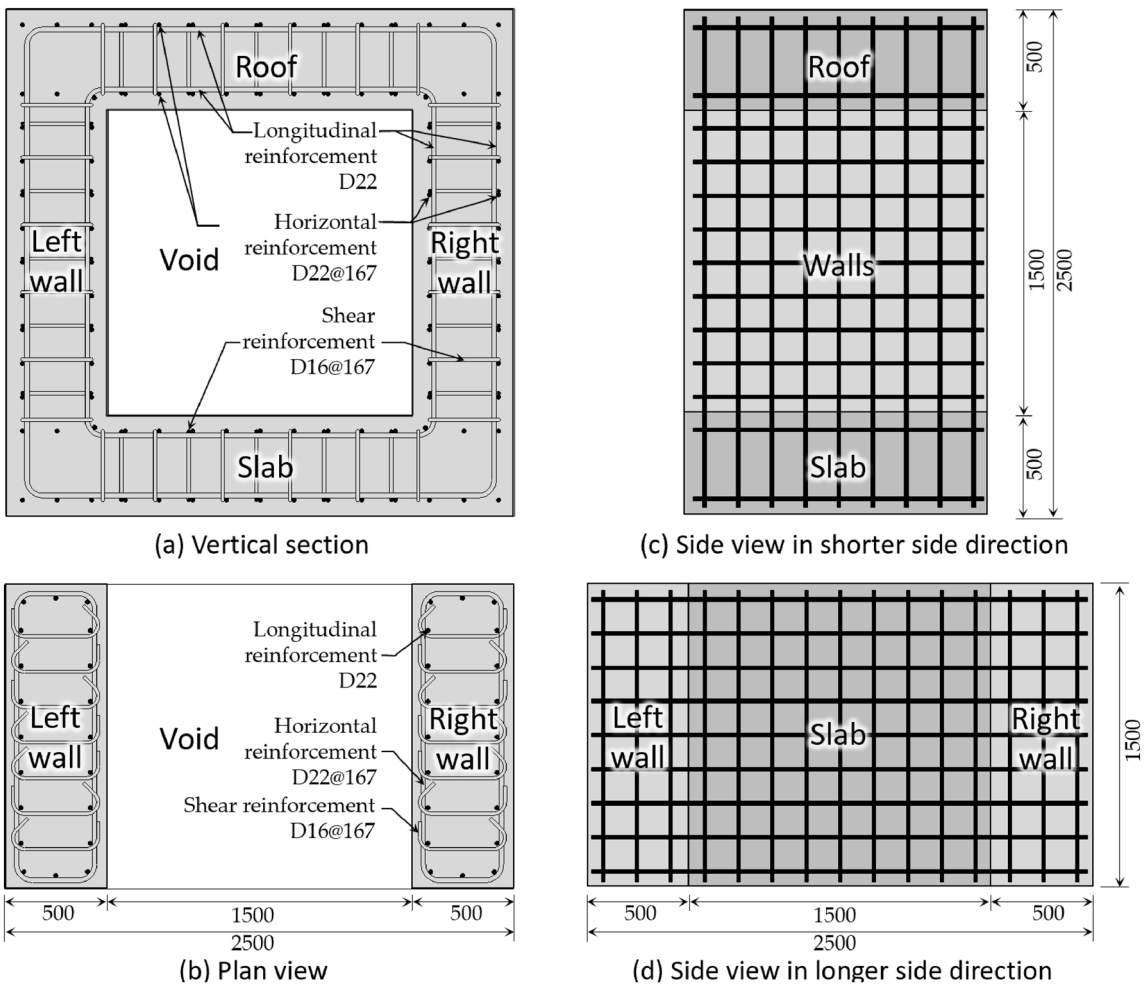

Fig. 2 Reinforcement details of Specimen HSC

Table 1 presents the test parameters of the specimens and Fig. 2 shows the dimensions and reinforcement details of the test specimens. The major parameter was the compressive strength of concrete (normal-strength concrete or high-strength concrete) and reinforcement ratio in the wall, slab, and roof. To ease constructability, a construction joint was located at the interface between the walls and slab. The ages of concrete at the slab, walls, and roof for normal-strength and high-strength concretes are presented in Table 1. Table 2 presents the mixture design for the normal-strength and high-strength concretes.

For longitudinal rebars, the minimum reinforcement according to DMFC 2–20–10 (Defense Installations Agency, 2014) was used, which is common practice in design of tunnels. Because the minimum reinforcement is a function of concrete strength, the vertical reinforcing bar ratio of Specimens NSC and HSC with normal-strength and high-strength concretes was determined as 0.306% (D16@175 mm) and 0.559% (D22@175 mm), respectively (Fig. 2a). The ratios of horizontal rebars were identical to those of vertical rebars. For the shear reinforcement to resist the internal pressure in the orthogonal direction, D16 was placed at a spacing of 175 mm both for Specimens NSC and HSC using the alternative hooks of 90° and 135° (Fig. 2b). Additional anchorages or stirrups can be reinforced for the wall–roof connection and wall–slab connection to provide greater tensile resistance and to prevent cracking addressing increased stress concentration near the corner. However, unconfined joints were primarily considered at the wall–roof connection and wall–slab connection for constructability in this test program.

2.2 Test Setup and Test Procedure

Prior to explosive test, three 100 mm × 200 mm cylinders were tested for compressive strength, according to ASTM C39M-20 (ASTM International, 2020). Three 200 mm × 200 mm × 600 mm rectangular prisms were tested for flexural strength in accordance with ASTM C78M-18 (ASTM C78 / C78M-18, 2018). To evaluate the mechanical properties of the reinforcing bars, three coupons were tested, according to ASTM E8M-16 (ASTM International, 2016). The yield strengths of the steel were defined using the 0.2% offset method for materials with unclear yield plateaus.

Fig. 1b shows the charge position and boundary conditions of the test. The test was performed at a blast training field in the Army Engineering School in Korea (Fig. 3a). As shown in Fig. 3b, the specimen was settled down to the ground excavated by the depth of 1.4 m. Prior to the settling down, the excavated ground was compacted with the distributed compaction sands so that the specimens stand flat on the ground. To simulate the confined internal space, the openings of the concrete structure were closed by steel plates with thickness of 5 mm. Then, soils were filled to temporarily support the internal explosive loading (Fig. 1b) from outer surfaces of the steel plates (Fig. 3c). Similar amount of soil was uniformly stacked at both ends of the specimens, for the internal pressure to act uniformly distributed to both ends of the specimen. Afterward, filling work was conducted using selected soil for the cover to simulate uniform soil pressure (Fig. 3d).

The two explosion tests were performed one by one: the first explosion for Specimen NSC and the second explosion for Specimen HSC. The second test was performed over time after the vibration of the soil was confirmed stabilized from the first explosion.

3 Test Result

3.1 Material Test Results

Table 3 shows the compressive strength, flexural strength, elastic modulus, and Poisson's ratio of concrete, measured at the day of test. Table 4 shows the yield strength f_y, tensile strength f_u, and tensile to yield strength ratio f_u/f_y of the reinforcing bars used in specimens.

3.2 Failure Modes

Fig. 4a and b shows the final failure modes of Specimens NSC and HSC at the end of test, respectively. In Specimen NSC, the roof of the structure was completely destroyed and blown out from the walls (Fig. 4a). It should be noted that the reinforcement of 0.25% was sufficient to carry the blast load generated at the scaled distance (1.43 to 1.45 m/kg$^{1/3}$) subjected to unconfined explosion according to previous study (Mendonça et al.,

Table 2 Concrete mix design of specimens

Target compressive strength (MPa)	W/C (%)	Unit weight (m/kg$^{1/3}$)							Slump (mm)	Maximum aggregate size (mm)
		W	C	FA	CA	FS	S	SP		
24	33.3	161	340	749	956	58	85	4.1	120	25
80	11.1	130	1026	1140	1075	114[†]			25	19

W = water, C = cement, FA = fine aggregate, CA = coarse aggregate, FS = fly ash, S = blast furnace slag, and SP = superplasticizer. [†]Each mix design of FS, S, and SP in the high-strength concrete used for the specimen is not disclosed due to trade secret by the concrete manufacturer

Fig. 3 Test setup

Table 3 Measured material properties of concrete used in specimens

Specimen	Compressive strength, MPa	Flexural strength, MPa	Elastic modulus, MPa	Poisson's ratio
NSC	26.7	4.9	20.31	0.22
HSC	100.8	13.3	44.72	0.18

Table 4 Measured material properties of reinforcing bar used in specimens

Reinforcing bars	Yield strength f_y, MPa	Tensile strength f_u, MPa	Tensile to yield strength ratio f_u/f_y
D16	459.7	565.0	1.23
D22	492.3	608.7	1.24

2017). In contrast, due to partially confined explosion with smaller scaled distance ($Z = 0.415$ m/kg$^{1/3}$), the minimum reinforcement ratio was not sufficient to provide blast resistance. Further, the failure surfaces were propagated throughout the wall–roof connection, which was not reinforced by confinement details in the specimen. Thus, further reinforcement details are necessary in the wall–roof and slab–roof connections considering the effects of partially confined explosion with smaller scaled distance.

However, in the case of Specimen HSC, diagonal crack occurred at the wall–roof connection and flexural cracks occurred along the span length of the roof (Fig. 4b). The roof was intact with the walls unlike Specimen NSC, owing to the increased concrete strength and reinforcement ratio. The test results indicate that in the case of 100 MPa high-strength concrete, the blowout of the roof can be resisted using the minimum reinforcement ratio subjected to scaled distance Z of 0.415 m/kg$^{1/3}$. Nevertheless, the diagonal cracking was severe due to stress concentration at the connection, which potentially leads to the blowout at the roof with further blast loadings. Therefore, special cautions are required for the confinement details in the wall–roof connections.

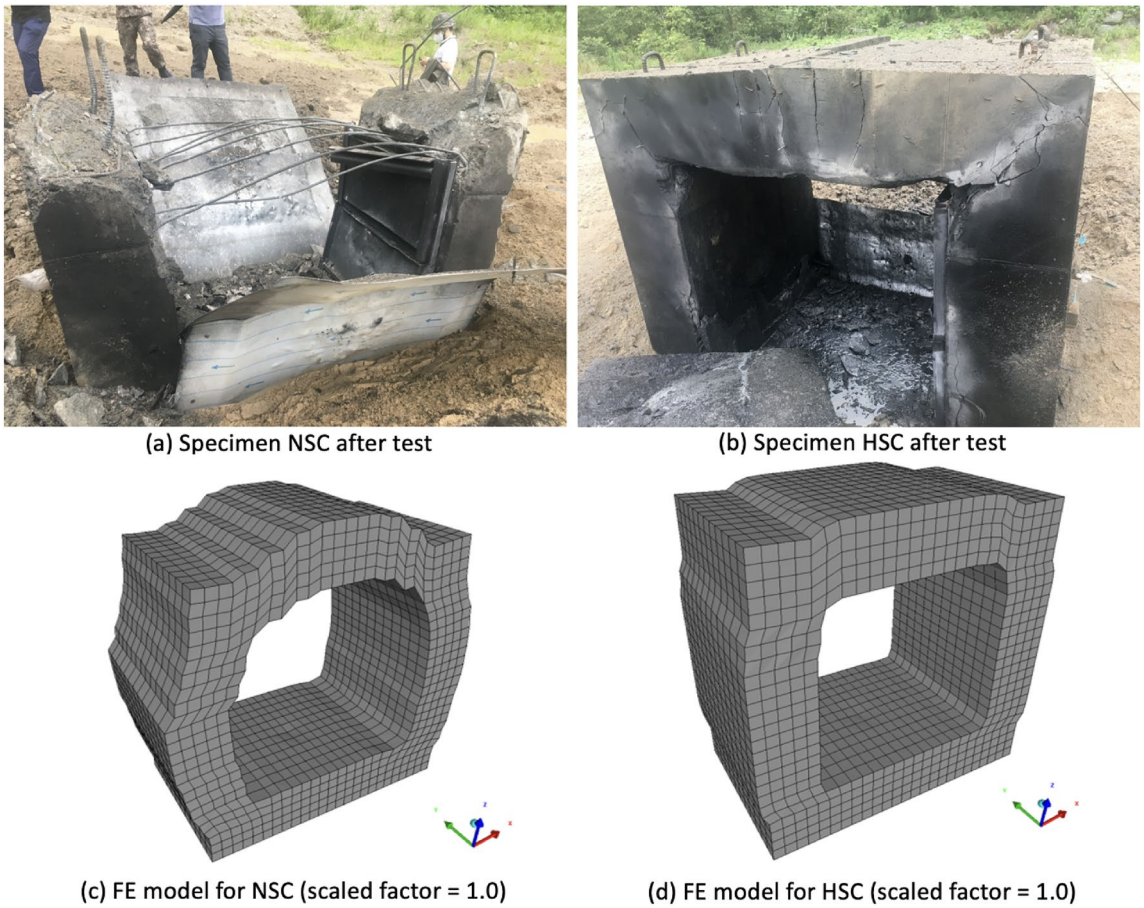

Fig. 4 Comparison of test specimen failure modes of FE model

4 Finite Element Analysis

4.1 Modeling and Calibration

The FE program AUTODYN was used to evaluate the effects of the partially confined explosion on the protective structure. Fig. 5 shows the section at the center of the FE model developed for the concrete structure and soil to simulate the test specimens. Using the symmetric condition of the test setup, only a quarter of specimen was modeled for calculation efficiency and a half of the whole specimen was visualized for convenience in the software.

The concrete, reinforcement, soil, and TNT enclosed by air were used for modeling the test specimen in the FE analysis (Fig. 5a). Eight-node solid elements were used for the concrete structure and soil materials. The mesh sizes of the concrete structure and soil were determined as 100 mm × 125 mm × 100 mm and 100 mm × 100 mm × 100 mm, respectively, by performing the sensitivity analysis until the error of FE analysis results with different mesh sizes became limited. The reinforcement material was embedded as a line element in the concrete material (Fig. 5). For concrete–reinforcement contact, no sliding or separation between the faces or edges is allowed, using option 'bonded' for 'Type reinforcement' in a function of the software. The purpose of the 5-mm-thick backfilling steel plate in the test was to prevent the backfilling soil particles from flowing into the structure (Fig. 3c). Because the soil elements in the FE analysis are not scattered unlike the test, the steel plate was simply not simulated (Fig. 5), assuming that the effect of the thin plate on the FE analysis result was negligible.

To simulate the TNT explosion, the TNT material with the charge weight of 5.9 kg equivalent to TNT used in the experiment enclosed by the air material was modeled using eight-node solid elements, which enables the Eulerian analysis. The shape of the TNT source was simulated as a cube like the experiment. The air element was modeled covering the concrete and soil elements (Fig. 5c) to simulate the explosion phenomenon as an ideal gas with a density of 1.225 kg/m^3 and adiabatic exponent (gamma) of 1.4. Considering the air and structure boundary conditions for the explosion analysis, the five surfaces excluding the bottom surface were set to flow out, and the

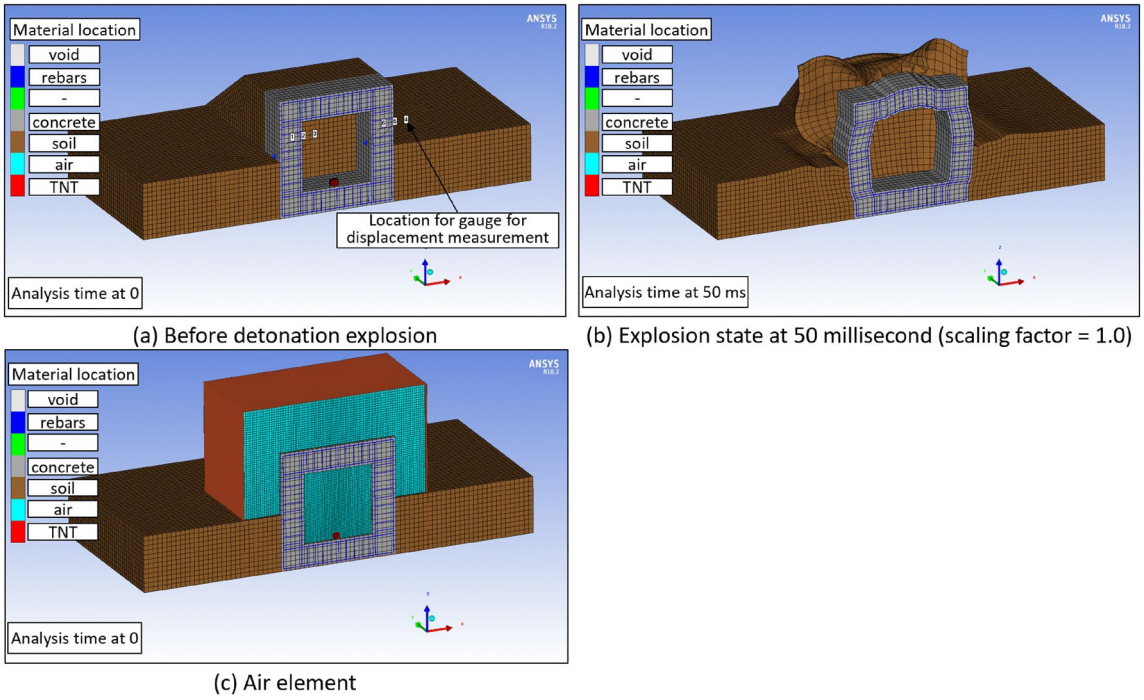

Fig. 5 Section view of FE model developed for the concrete structure and soil

bottom surface was set to reflection with a coefficient of 1.8 to address the consequent energy losses of ground displacement. To avoid convergence issue, the mesh sizes of the TNT and air elements were relatively smaller than those of Lagrangian analysis for concrete structure and soil, which varied from 25 mm × 25 mm × 25 mm in the TNT center to 45 mm × 45 mm × 50 mm in the outer surface of the air, using zoning function implemented in the FE software. The mesh sizes were determined considering the better accuracy and less time consumed for the FE analysis.

Table 5 presents the structural specifications and material properties used in FE model. There are several material options provided to model the concrete structures and soil for the modeling of the structure elements in AUTODYN. In this study, a Riedel–Hiermaier–Thoma (RHT) dynamic damaged concrete model (Riedel et al., 1999) that takes into account strain hardening and the third invariant dependence was applied to represent the behavior of concrete under blast loads. The RHT model consists of three strength surfaces defined as a failure surface, elastic limit surface, and residual surface. The elastic strength surface can express the material strain hardening behavior and the residual strength surface can address the strength of fully crushed concrete under the ultimate blast load. The constitutive relation of concrete model was considered as a quasi-brittle material with different behaviors in tension and compression.

Table 5 Material properties used in FE model

Material	Parameter	
Normal-strength concrete	Compressive strength	26.7 MPa
	Tensile strength	2.4 MPa
	Shear strength	4.32 MPa
	Shear modulus	1.48×10^4 MPa
	Bulk modulus	3.21×10^4 MPa
	Density	2,304 kg/m^3
High-strength concrete	Compressive strength	100.8 MPa
	Tensile strength	8 MPa
	Shear strength	14.4 MPa
	Shear modulus	2.47×10^4 MPa
	Bulk modulus	5.52×10^4 MPa
	Density	2,441 kg/m^3
Soil (The Drucker–Prager model)	Shear modulus	7.85×10^3 MPa
	Bulk modulus	2.07×10^3 MPa
	Density	1,920 kg/m^3
	Poisson's ratio	0.332
Air	Density	1.225 kg/m^3
	Gamma	1.40
	Initial internal energy	206,800 kJ/kg
TNT	Density	1.630
	Detonation velocity	6.93×10^3 m/s
	Energy/unit volume	6.00×10^6 kJ/m^3
Global erosion by geometric strain		1.5

Several material options for the soil are also available in AUTODYN. These material options range from elastic material to a non-linear material option. In this study, the Drucker–Prager model was applied to present the behavior of the soil during blast loading. The Drucker–Prager criterion has the smooth surface in the stress space, which results in easier implementation of the criterion and enables the analysis of the mechanical properties of soil. The Drucker–Prager model in AUTODYN is elastic and perfectly plastic material having only one surface. The concrete fracture is simulated by the element erosion techniques, which have been studied to define precise erosion criterion (Codina et al, 2016, Galuta and Wafa, 2018; Luccioni & Gabriel, 2011; Luccioni et al., 2013; Luccioni et al., 2018; Tu & Lu, 2009). In this study, the global erosion parameter based on geometric strain implemented in AUTODYN was determined as 1.5 in accordance with experience and recommendation from previous studies.

The contact condition for concrete wall-backfilling soil was frictionless. The cohesion provided in the FE analysis for the frictionless contact (i.e., concrete wall-backfilling soil) was 0, which allows for the separation of the backfilling soil from the concrete wall under explosion. The provided friction angle was 38°, which is a general value for compacted sands.

The applicability of the FE model developed to predict the partially confined explosion phenomenon was evaluated. In this study, a comparison was made between the results from the field experiment and the FE model developed. The results confirmed that the failure mode during the explosion predicted by FE model developed was well matched with those calculated using the FE model as shown in Fig. 4. However, the measured displacement was lost and unrecorded during explosion due to malfunction of the sensors. Because the parameters for the FE analysis was not able to calibrate based on the test, it should be noted that only qualitative comparison was performed in the following parametric study.

4.2 Parametric Study Results

In order to investigate the effective protection method against explosion, the parametric study under three different confined explosion conditions including fully vented, partially confined, and fully confined explosion defined in UFC 3-340-02 (Han et al., 2018) was conducted. Fig. 6 shows the section at the center of the FE model developed for the parametric study. Like the FE model simulating the test specimen (Fig. 5a), the symmetric condition was used for calculation efficiency. The fully vented explosion condition was implemented by removing backfilling soil elements from the FE model used for the test specimens (Fig. 6a). To simulate the air ventilation through the openings, the boundary condition of the air element was set to 'flow out' in the FE program. The fully confined condition was simply implemented by modeling the confined air element within the tunnel, which simulates the complete reflection condition of the internal space (Fig. 6b). Contrary to the fully vented or fully confined explosion conditions, the partially confined explosion conditions may be extremely varied according to the degree of the explosion confinement. In this study, the FE model simulating the test specimen (Fig. 5a) was used for comparison. Like the test

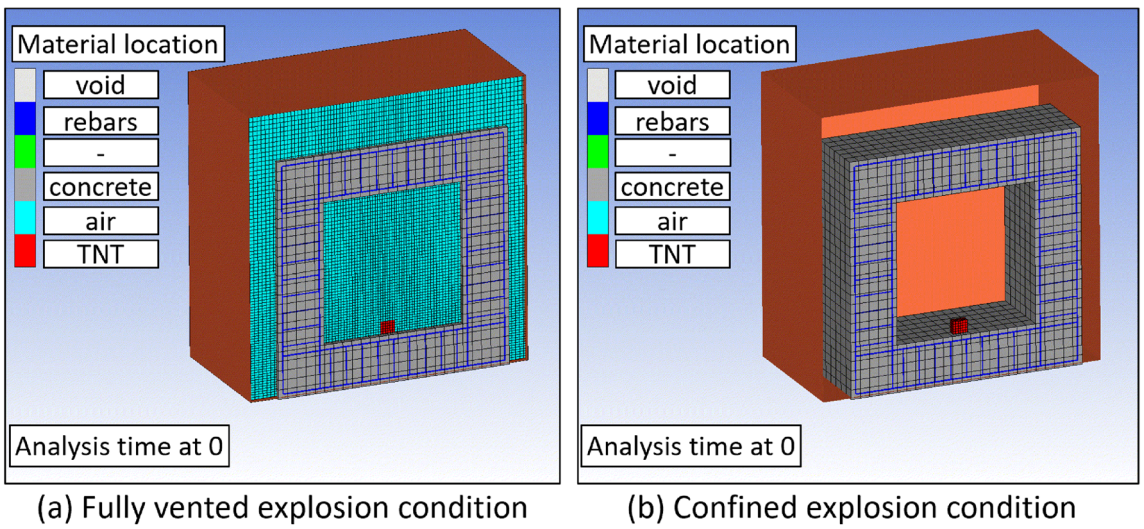

Fig. 6 Section view of FE models developed for the parametric study

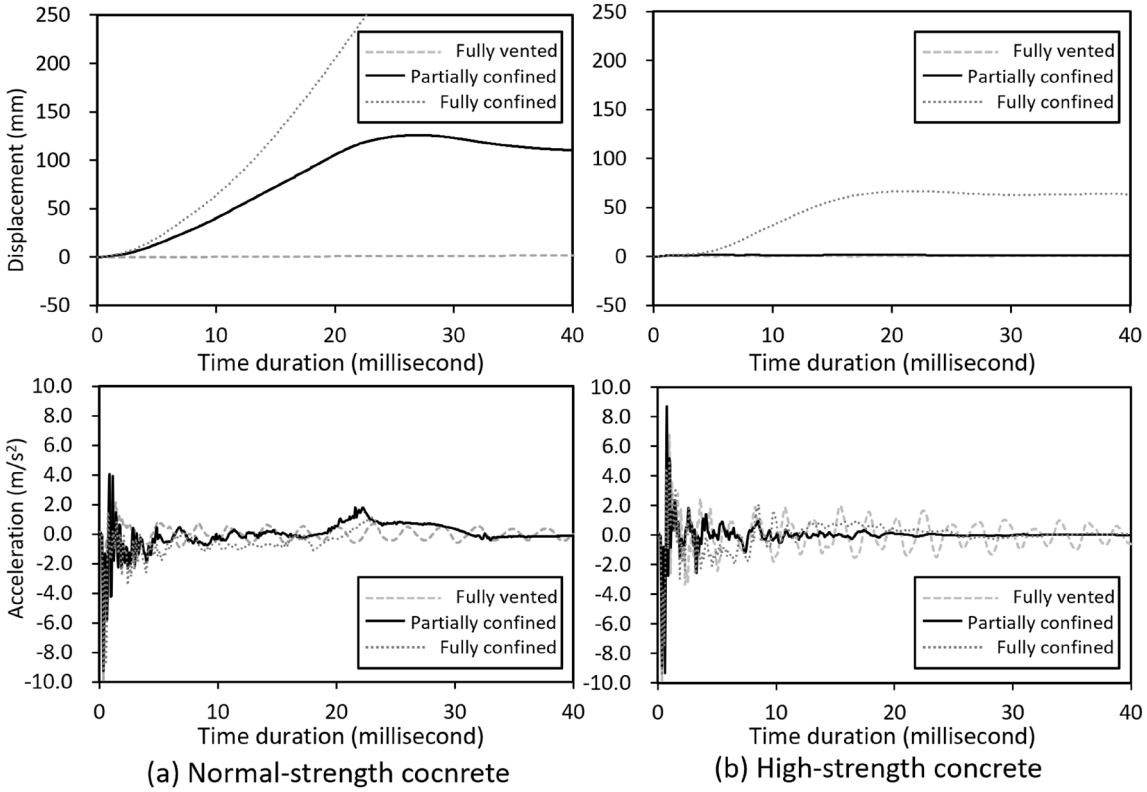

Fig. 7 Displacement and acceleration calculated at outer surface of wall with different confinement conditions in FE analysis results

Table 6 Maximum displacement at outer wall (or roof) center of Specimens NSC and HSC calculated at the end of FE analysis under fully vented, partially confined, and fully confined explosion conditions

Specimen	Explosion condition	Wall (mm)	Roof (mm)
NSC	Fully vented	1.414	1.315
	Partially confined	125.938	-
	Fully confined	262.514	334.617
HSC	Fully vented	0.643	0.681
	Partially confined	1.712	-
	Fully confined	66.841	98.920

specimens, the concrete strength with its minimum reinforcement ratio was used as a FE analysis parameter.

Fig. 7 shows the displacement and acceleration at outer surface of the wall during explosion under three different explosion conditions. The location of the gauge for the displacement and acceleration is shown in Fig. 5. Table 6 presents the maximum displacement calculated by explosion under different explosion conditions at the measured point (gauge #4 in Fig. 5a). The calculated acceleration in high-strength concrete was greater than that of normal-strength concrete, whereas the calculated displacement in high-strength concrete was smaller than that of normal-strength concrete. The calculated displacement, which is used for design, was used for the comparison rather than acceleration.

With the analysis time increased, the displacement of the wall increased as shown in Fig. 7. The displacements were greatest under the fully confined explosion in both the FE models with normal-strength and high-strength concretes. The extremely large displacement implies the complete failure of the wall from the structure. However, by using high-strength concrete, the maximum displacement was significantly reduced to approximately a quarter (66.8 mm), when compared to that of normal-strength concrete (262.5 mm). This result implies that building a protective structure against fully confined explosion requires high-strength concrete with fine-detailed reinforcement.

On the other hand, under the fully vented explosion condition, small deformation occurred in both the FE models with normal- and high-strength concretes. The negligible damage to the structure regardless of the concrete strength conversely indicates a full transfer of the explosion load to the surroundings (e.g., people around the explosion), which implies that under fully vented

explosion condition, a structure may be ineffective as a protective measure.

Under partially confined explosion condition, the calculated displacement in the FE model was smaller than fully confined model and was greater than fully vented model. The reduction of the maximum displacement by using higher concrete strength ((125.93—1.71) mm / 125.93 mm = 98.7%) was even greater than that under fully confined model ((262.514—66.842) mm / 262.514 mm = 74.5%). Since the leakage pressures and impulse are a function of the vent area divided by the structure volume, it is possible to reduce the blast pressure while preventing the destruction of the structure with adequate strength of materials.

5 Conclusion

In this study, to investigate the resistance of structures containing explosive materials such as ammunition in military or hydrogen tanks in private sector, partially confined explosion tests were performed. Two reinforced concrete structures were tested subjected to a charge weight of 5.9 kg TNT explosion. Tunnel-type reinforced concrete structures with thickness of 0.5 m were fabricated and were covered by thin steel plates and backfilling soil to simulate the partially confined explosion in a structure before TNT detonation in the slab center. The major parameter was the compressive concrete strength (26.7 and 100.8 MPa) with minimum horizontal and vertical rebar ratio (0.306 and 0.559%) in roof and walls. The failure modes of specimens with normal- and high-strength concretes were compared. Further, the FE program AUTODYN software was used to evaluate the effects of the different explosion conditions on the protective structure. The major findings of this study were summarized as follows:

1. Although a minor cracking was expected by the design of Technical Manual 5–855 (Army, 1986) in the specimen with normal-strength concrete and minimum reinforcement ratio, the partially confined concrete structure was completely failed by the roof blowout, due to the absence of the wall–roof confinement hoops. It is necessary for partially confined concrete structure to install further reinforcement details in the wall–roof and slab–roof connections.
2. On the contrary, in the specimen with high-strength concrete and minimum reinforcement ratio, the roof–wall connection was relatively mild and was intact with the adjacent walls, despite the absence of the confinement hoops. This result indicates that the increase in concrete strength can be effective in improving protective structures under partially confined explosion.
3. The parametric study using the FE program was conducted under fully confined, fully vented, and partially confined explosions. Under fully confined explosion, the displacements were extremely large. However, by using higher-strength concrete, the maximum displacement was significantly reduced to approximately a quarter. This result implies that high-performance materials are required for a protective structure under fully confined explosion, with extremely large internal overpressure.
4. Under fully vented explosion, the displacement was negligible due to full pressure leakage through venting, which is ineffective as a protective structure.
5. Under partially confined explosion, the use of the higher concrete strength reduced the maximum displacement by 98.7%. The results indicate that it is possible to reduce the blast pressure effects by controlling the degree of the explosion confinement and by using adequate strength of materials, while preventing the destruction of the structure.
6. This study provides experimental concrete damages and FE analysis results under a certain case of the partially confined explosion. For designing the facilities with explosives such as ammunition storage or hydrogen charging station in military facilities and civilians, further experimental research is required to investigate more various degree of explosion confinement. Furthermore, different levels of reinforcement details, such as maximum reinforcement ratio in member and more confinement in wall–roof connection, should be investigated.

Acknowledgements

This work was supported by a grant from National Research Foundation of Korea (NRF) funded by the Korean government (MSIT) (RS-2023-00218832) and by a grant from Kyung Hee University in 2021 (KHU-20211888). This work was also supported by the Korea Institute of Energy Technology Evaluation and Planning (KETEP) and the Ministry of Trade, Industry & Energy (MOTIE) of the Republic of Korea (No. 20215810100020). The authors would like to thank Army Engineering School in Korea for supporting this research with the explosives, sites, and measurements for detonation test.

Author contributions

J-WB contributed to conceptualization, methodology, supervision, funding acquisition, and writing—original draft; YP was involved in writing—original draft preparation, investigation, validation, and visualization and provided software; S-WP, KK, and S-GY provided software and performed project administration and writing—review and editing; KK was responsible for data curation and writing—review and editing. All authors have read and agreed to the published version of the manuscript.

Funding

This work was supported by a grant from National Research Foundation of Korea (NRF) funded by the Korean government (MSIT) (RS-2023-00218832) and by a grant from Kyung Hee University in 2021 (KHU-20211888). This work was also supported by the Korea Institute of Energy Technology Evaluation and Planning (KETEP) and the Ministry of Trade, Industry & Energy (MOTIE) of the Republic of Korea (No. 20215810100020).

Data availability
The data that support the findings of this study are available from the corresponding author, J.-W. Baek, upon reasonable request.

Declarations

Competing interests
The authors declare that they have no known competing financial interests or personal relationships that could have appeared to influence the work reported in this paper.

Received: 8 February 2023 Accepted: 11 January 2024
Published online: 06 June 2024

References

Army U (1986). Fundamentals of protective design for conventional weapons. Technical manual TM 5–855, Dept. of the Army, Washington DC, USA

ASTM International (2016). Standard Test Methods for Tension Testing of Metallic Materials: ASTM E8 / E8M - 16," ASTM International, West Conshohocken, PA, USA

ASTM C78 / C78M-18 (2018). Standard Test Method for Flexural Strength of Concrete (Using Simple Beam with Third-Point Loading). ASTM International, West Conshohocken, PA, USA

ASTM International (2020). Standard Test Method for Compressive Strength of Cylindrical Concrete Specimens: ASTM C39 / C39M-20. ASTM International, West Conshohocken, PA, USA

Buhin, L. (2016). Integrated Cooperation on Explosive Hazards Program in Central Asia. *Journal of Conventional Weapons Destruction, 20*(2), 8.

Chen, Y., Wu, X., Zheng, J., Deng, G., & Li, Q. (2010). Dynamic responses of discrete multi-layered explosion containment vessels with the consideration of strain-hardening and strain-rate effects. *International Journal of Impact Engineering, 37*(7), 842–853. https://doi.org/10.1016/j.ijimpeng.2009.11.011

Choi, M. (2009). Direction of military environment and construction project. Master Thesis, Kyongwon University, Kyonggi, Korea

Codina, R., Daniel, A., & Fernanda, B. (2016). Experimental and numerical study of a RC member under a close-in blast loading. *Engineering Structures, 127*, 145–158. https://doi.org/10.1016/j.engstruct.2016.08.035

Defense Installations Agency (2014). Department Military Facilities Criteria 2–20–10: Design Criteria for explosion-proof and bullet-proof facilities. Ministry of National Defence of Korea, Korea

Dong, Q., Li, Q., & Zheng, J. (2010). Further study on strain growth in spherical containment vessels subjected to internal blast loading. *International Journal of Impact Engineering, 37*(2), 196–206. https://doi.org/10.1016/j.ijimpeng.2009.09.001

Edri, I., Feldgun, V., Karinski, Y., & Yankelevsky, D. (2012). On blast pressure analysis due to a partially confined explosion: III. Afterburning effect. *International Journal of Protective Structures, 3*(3), 311–331. https://doi.org/10.1260/2041-4196.3.3.311

Edri, I., Savir, Z., Feldgun, V., Karinski, Y., & Yankelevsky, D. (2011). On blast pressure analysis due to a partially confined explosion: I. Experimental studies. *International Journal of Protective Structures, 2*(1), 1–20. https://doi.org/10.1260/2041-4196.2.1.1

Feldgun, V., Karinski, Y., Edri, I., Tsemakh, D., & Yankelevsky, D. (2012). On blast pressure analysis due to a partially confined explosion: II. numerical studies. *International Journal of Protective Structures, 3*(1), 61–79. https://doi.org/10.1260/2041-4196.3.1.61

Feldgun, V., Karinski, Y., Edri, I., & Yankelevsky, D. (2016). Prediction of the quasi-static pressure in confined and partially confined explosions and its application to blast response simulation of flexible structures. *International journal of impact engineering, 90*, 46–60. https://doi.org/10.1016/j.ijimpeng.2015.12.001

Feldgun, V., Karinski, Y., & Yankelevsky, D. (2011). Some characteristics of an interior explosion within a room without venting. *Structural Engineering and Mechanics, 38*(5), 633. https://doi.org/10.12989/sem.2011.38.5.633

Galuta, E., & Wafa, R. (2018). Numerical simulations of RC panels subjected to high speed projectile-erosion selection in AUTODYN-3D code. *International Journal of Innovative Science, Engineering & Technology, 4*(8), 25–30.

Han, U., Oh, J., & Lee, H. (2018). Safety investigation of hydrogen charging platform package with CFD simulation. *International Journal of Hydrogen Energy, 43*(29), 13687–13699. https://doi.org/10.1016/j.ijhydene.2018.05.116

Hu, H. T., & Lin, Y.-H. (2006). Ultimate analysis of PWR prestressed concrete containment subjected to internal pressure. *International Journal of Pressure Vessels and Piping, 83*(3), 161–167. https://doi.org/10.1016/j.ijpvp.2006.02.030

Hung, C.-W., Lai, H.-H., Shen, B.-C., Wu, P.-W., & Chen, T.-A. (2020). Development and validation of overpressure response model in steel tunnels subjected to external explosion. *Applied Sciences, 10*(18), 6166. https://doi.org/10.3390/app10186166

Kim, K., & Park, Y. (2020). Development of design considerations as a sustainability approach for military protective structures: A case study of artillery fighting position in South Korea. *Sustainability, 12*(16), 6479. https://doi.org/10.3390/su12166479

Liang, Y., Pan, X., Zhang, C., Xie, B., & Liu, S. (2019). The simulation and analysis of leakage and explosion at a renewable hydrogen refuelling station. *International Journal of Hydrogen Energy, 44*(40), 22608–22619. https://doi.org/10.1016/j.ijhydene.2019.05.140

Liao, Z., Tang, D., Li, Z., Xue, Y., & Shao, L. (2019). Study on explosion resistance performance experiment and damage assessment model of high-strength reinforcement concrete beams. *International Journal of Impact Engineering, 133*, 103362. https://doi.org/10.1016/j.ijimpeng.2019.103362

Lin, C.-P., Chang, C.-P., Chou, Y.-C., Chu, Y.-C., & Shu, C.-M. (2010). Modeling solid thermal explosion containment on reactor HNIW and HMX. *Journal of Hazardous Materials, 176*(1–3), 549–558. https://doi.org/10.1016/j.jhazmat.2009.11.064

Lin, R. H., Ye, Z.-Z., & Wu, B.-D. (2020). A review of hydrogen station location Smart Construction Research Group, Hyundai Engineering and Construction, Seoul 03508, South Korea models. *International Journal of Hydrogen Energy, 45*(39), 20176–20183. https://doi.org/10.1016/j.ijhydene.2019.12.035

Luccioni, B., & Gabriel, A. (2011). Erosion criteria for frictional materials under blast load. *Mecánica Computacional., 30*(21), 1809–1831.

Luccioni, B., Gabriel, A., & Nicolás, L. (2013). Defining erosion limit for concrete. *International Journal of Protective Structures, 4*(3), 315–340.

Luccioni, B., Isla, F., Codina, R., Ambrosini, D., Zerbino, R., Giaccio, G., & Torrijos, M. C. (2018). Experimental and numerical analysis of blast response of high strength fiber reinforced concrete slabs. *Engineering Structures, 175*, 113–122. https://doi.org/10.1016/j.engstruct.2018.08.016

Mendonça, F., Urgessa, G. S., Rocco, J. (2017), Blast Response of 60 MPa Reinforced Concrete Slabs Subjected to Non-Confined Plastic Explosives, Structures Congress 2017, Denver., American Society of Civil Engineers. p. 15–26. https://doi.org/10.1061/9780784480397.002

Mendonça, F., Urgessa, G., & Rocco, J. (2018b). Experimental investigation of 50 MPa reinforced concrete slabs subjected to blast loading, Ingeniería e Investigación, 38(2), 27–33. https://doi.org/10.15446/ing.investig.v38n2.65305

Mendonça, F., Urgessa, G., Iha, K., Rocha, R., & Rocco, J. (2018a). Comparison of Predicted and Experimental Behaviour of RC Slabs Subjected to Blast using SDOF Analysis. Defence Science Journal, 68(2), 138–143. https://doi.org/10.14429/dsj.68.11682c

Mendonça, F., Urgessa, G. S., Almeida, L., & Rocco, J. (2021). Damage diagram of blast test results for determining reinforced concrete slab response for varying scaled distance, concrete strength and reinforcement ratio. *Anais Da Academia Brasileira De Ciências, 93*, e20200511. https://doi.org/10.1590/0001-3765202120200511

Moradi, R., & Groth, K. M. (2019). Hydrogen storage and delivery: Review of the state of the art technologies and risk and reliability analysis. *International Journal of Hydrogen Energy, 44*(23), 12254–12269. https://doi.org/10.1016/j.ijhydene.2019.03.041

Pandey, A., Kumar, R., Paul, D., & Trikha, D. (2006). Non-linear response of reinforced concrete containment structure under blast loading. *Nuclear Engineering and Design, 236*(9), 993–1002. https://doi.org/10.1016/j.nucengdes.2005.09.015

Remennikov, A. M., & Rose, T. A. (2005). Modelling blast loads on buildings in complex city geometries. *Computers & Structures, 83*(27), 2197–2205. https://doi.org/10.1016/j.compstruc.2005.04.003

Riedel, W., Thoma, K., Hiermaier, S., & Schmolinske, E. (1999). Penetration of reinforced concrete by BETA-B-500 numerical analysis using a new macroscopic concrete model for hydrocodes. Proceedings, Proceedings of the 9th International Symposium on the Effects of Munitions with Structures, May 3–7, Berlin-Strausberg, Germany

Smith, P. D., & Rose, T. A. (2006). Blast wave propagation in city streets—an overview. *Progress in Structural Engineering and Materials, 8*(1), 16–28. https://doi.org/10.1002/pse.209

Tu, Z., & Lu, Y. (2009). Evaluation of typical concrete material models used in hydrocodes for high dynamic response simulations. *International Journal of Impact Engineering, 36*(1), 132–146. https://doi.org/10.1016/j.ijimpeng.2007.12.010

UFC (2008). Unified Facilities Criteria 3–340–02: Structures to resist the effects of accidental explosions. Dept. of the Army, the NAVY and the Air Force, Washington DC, USA

Wang, W., Zhang, D., Lu, F., Wang, S.-C., & Tang, F. (2012). Experimental study on scaling the explosion resistance of a one-way square reinforced concrete slab under a close-in blast loading. *International journal of impact engineering, 49*, 158–164. https://doi.org/10.1016/j.ijimpeng.2012.03.010

Wang, W., Zhang, D., Lu, F., Wang, S.-C., & Tang, F. (2013). Experimental study and numerical simulation of the damage mode of a square reinforced concrete slab under close-in explosion. *Engineering Failure Analysis, 27*, 41–51. https://doi.org/10.1016/j.engfailanal.2012.07.010

Zhao, C., Chen, J., Wang, Y., & Lu, S. (2012). Damage mechanism and response of reinforced concrete containment structure under internal blast loading. *Theoretical and Applied Fracture Mechanics, 61*, 12–20. https://doi.org/10.1016/j.tafmec.2012.08.002

Zhi, X.-D., Qi, S.-B., & Fan, F. (2019). Temporal and spatial pressure distribution characteristics of hemispherical shell structure subjected to external explosion. *Thin-Walled Structures, 137*, 472–486. https://doi.org/10.1016/j.tws.2019.01.021

Publisher's Note

Youngjun Park is an Vice President in the Technical Research Center at Hyundai Engineering and Construction, Seoul, South Korea. He received his BE in the Department of Civil Engineering at the Korea Military Academy and PhD in the Civil and Coastal Engineering at the University of Florida. His research interests include design and behavior of the protective structures against weapon system and smart construction based on the AI and Big-data.

Kukjoo Kim is a Protective Structure Analyst in the Protective Design Division of Defense Installations Agency, Seoul, South Korea. He received his BE in the Department of Civil Engineering at Korea Military Academy. He also received a MS in Civil Engineering at the Texas A&M University and a Ph.D. from the University of Florida. His research interests include design and behavior of protective structures against blast loads.

Sang-woo Park is an Associate Professor in the Department of Civil Engineering & Environmental Science at Korea Military Academy, Seoul, South Korea. He received his BE and PhD in the School of Civil, Environmental & Architectural Engineering at Korea University. His research interests include the performance evaluation of protective technologies and the design of underground protective structures.

Sang-Guk Yum is currently an Assistant Professor in the faculty of Department of Civil Engineering at Gangneung-Wonju University (GWNU) in South Korea. He earned his Master of Science degree from Texas A&M University and obtained his Ph.D. in Civil Engineering and Engineering Mechanics from Columbia University. He has a substantial publication record in reputable journals and has actively contributed to academic research in construction management and risk analysis, with a focus on construction safety. Additionally, he has presented numerous academic and research-based papers at both national and international conferences.

Jang-Woon Baek is an Assistant Professor in the Department of Architectural Engineering at Kyung Hee University, Gyeonggi, South Korea. He received his BE, MS, and PhD in the Department of Architecture & Architectural Engineering at Seoul National University. His research interests include design and behavior of shear walls under seismic or blast loads.